

Original Article

Reliability of cone counts using an adaptive optics retinal camera

Mélanie Bidaut Garnier MD,¹ Mathieu Flores MD,¹ Guillaume Debellemanière MD,¹ Marc Puyraveau MSc,² Perle Tumahai MD,¹ Mathieu Meillat MD,¹ Claire Schwartz MD,¹ Michel Montard MD PhD,¹ Bernard Delbosc MD PhD¹ and Maher Saleh MD PhD¹

¹Department of Ophthalmology and ²Center of Clinical Methodology, University Hospital of Besançon, University of Franche-Comté, Besançon, France

ABSTRACT

Background: To assess the reproducibility and repeatability of cone imaging in healthy human eyes, using the RTx-1 Adaptive Optics Retinal Camera and its proprietary cone-counting software.

Design: Single-centre, prospective study.

Participants: Ten healthy adults.

Methods: Macular cones were imaged. Intrasession repeatability was assessed by comparing 10 consecutive acquisitions obtained by the same operator from each subject. For the intersession study, each subject was imaged five consecutive days. Interoperator reproducibility was also evaluated by comparing the images obtained from 10 different subjects by two independent operators. Finally, intergrader agreement was evaluated by comparing the cone counts measured by two masked graders.

Main Outcome Measures: Mean cone density (cells/mm²), spacing between cells (μm) and percentage of cones with six neighbours calculated on Voronoi diagrams were measured. Correlation coefficients, intraclass correlation coefficients, and coefficients of variation were calculated.

Results: Correlation coefficient and intraclass correlation coefficient were respectively 0.81 and 0.96 between operators, and 0.97 and 0.98 between the

two graders. The intrasession and intersession coefficients of variation were under 7%. The percentage of cells with six neighbours and the spacing between cones varied in the same proportion (coefficients of variation ranged from 1.66 to 10.05%).

Conclusions: Overall, the test–retest variability of RTx-1 and its software was good in normal human eyes. Further studies in the normal clinical setting are mandatory.

Key words: cell count, healthy volunteers, optical imaging, reproducibility of results, retinal cone photoreceptor cells.

INTRODUCTION

Adaptive optics (AO) retinal imaging, which uses active optical elements to compensate for aberrations in the optical path between the retina and the camera, allows high magnification and real-time visualization of the macular cones.¹ This new imaging modality has been increasingly used in vision research to study the mosaic and alignment of cones and the retinal vasculature.^{1–7}

Because the AO system has been shown to image the retina with a level of detail not seen with other imaging instruments such as optical coherence tomography and scanning laser ophthalmoscopy, a growing interest in its potential use in clinical ophthalmology has been observed. For example, applications in frequent macular conditions such

■ **Correspondence:** Dr Maher Saleh, Department of Ophthalmology, University Hospital of Besançon, University of Franche-Comté, CHU Jean Minjot, 3 boulevard Alexandre Fleming, 25030 Besançon, France. Email: msaleh@chu-besancon.fr

Received 15 December 2013; accepted 15 April 2014.

Competing/conflicts of interest: No stated conflict of interest.

Funding sources: No stated funding sources.

as epimacular membrane,^{8,9} macular hole^{10,11} and age-related macular degeneration^{12–14} have been recently reported. The development of the first commercially available compact AO retinal camera device (i.e. the RTX-1, Imagine Eye, Orsay, France) may accelerate the transfer of AO from fundamental research to clinical practice. However, data on the reliability and robustness of the measurements taken with AO are scarce compared to other retinal imaging techniques such as optical coherence tomography.^{15–22} While the reliability of AO coupled with a scanning laser ophthalmoscopy system (AOSLO)^{23–25} has been studied, data on the reliability of the RTX-1 are rare.⁶

In this study, we investigated the repeatability and reproducibility of cone counting using the RTX-1 and its dedicated software in a healthy population, in order to provide a base point for comparison for upcoming studies conducted on patients.

METHODS

Subjects

Ten healthy volunteers were recruited in our department of ophthalmology. All subjects underwent a comprehensive eye examination. None had any history of ocular or systemic disease, and they all displayed the best corrected visual acuity of 20/20 or better. Dry eye, retinal or systemic diseases were exclusion criteria. In accordance with the Helsinki declaration, written consent was obtained after explaining the goal and design of the study as well as the imaging modality and its consequences.

RTX-1 specifications and image acquisition procedure

Cones were imaged using the RTX-1 AO retinal camera, from Imagine Eyes (Orsay, France). This device, approved for research use only in Europe, is a non-contact en-face imaging device using non-coherent flood illumination with a wavelength of 850 nm. Aberrations of the ocular wavefront are analyzed by an integrated aberrometer, with a Shack–Hartmann wavefront sensor. Aberrations are corrected by a deformable mirror in real time. Imaging field of view is $4^\circ \times 4^\circ$, corresponding to a 1.2×1.2 mm square on the retinal surface. Each acquisition lasts 4 s. Its low-noise charge-coupled device camera has a pixel resolution of $1.6 \mu\text{m}$ and a frame rate of 9.5 fps.

AO imaging sessions, were conducted on undilated subjects at a fixed time (9 a.m.) by trained operators. The head was positioned on the chinrest at a working distance of 50 mm while the subject fixed his or her gaze on a target (a yellow cross) located inside the device. The area of the retina to be imaged

was chosen by adjusting the position of the fixation target horizontally, the imaging depth was chosen within the range of 0 to $-80 \mu\text{m}$; in this range, the live images of the retina appeared to be the sharpest ($-800 \mu\text{m}$ and $+800 \mu\text{m}$ correspond to the anterior and posterior retina, respectively). During the acquisition, a numerical value in the device's control panel informed the operator on the level of OA correction in real time: the lower this value was the better the correction and thus the better the acquisition quality. During the acquisition, 40 live high-resolution images of the retina were automatically averaged by the device in a single session.

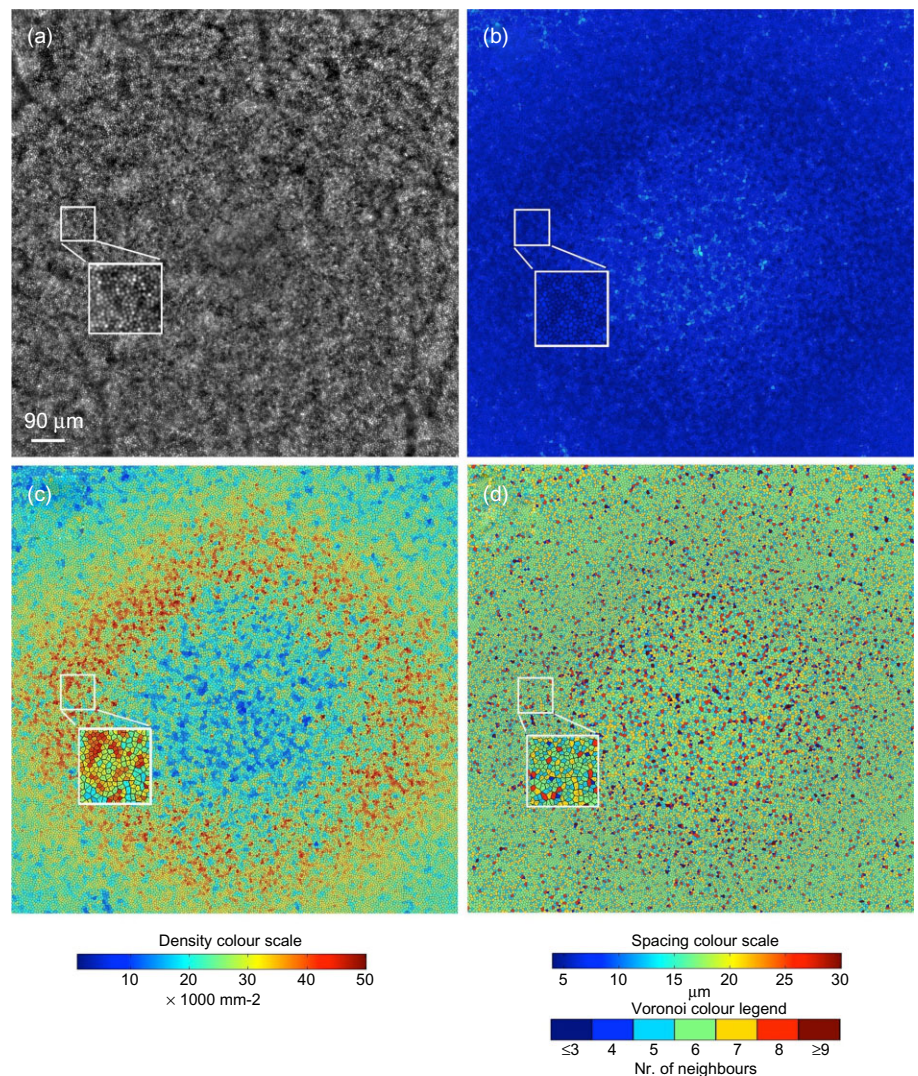
Image processing and analysis

Each series of 40 images acquired by the AO camera was processed using software programs provided by the system manufacturer (CK v0.1 and AOdetect v0.1, Imagine Eyes). These images were registered using a cross-correlation method^{26,27} and averaged to produce a final image with improved signal-to-noise ratio. The raw images that showed artefacts due to eye blinking and saccades were automatically eliminated before averaging. For display and printing purposes, the background of the resulting image was subtracted using a Gaussian filter, and the histogram was stretched over a 16-bit range of gray levels. The positions of photoreceptors were computed by automatically detecting the central coordinates of small circular spots whose brightness was higher than the surrounding background level.

First, the averaged image, as obtained before background removal and histogram stretching, was further processed using adaptive²⁸ and multiple-scale²⁹ digital filters. Then, the local maxima of the resulting filtered image were deleted and their pixel coordinates were recorded.

The spatial distribution of these point coordinates was finally analyzed in terms of inter-cell spacing (μm), local cell density (cells/ mm^2) and number of nearest neighbours corresponding of the percentage of cells with six neighbours (P6) using Delauney triangulation³⁰ and calculated on Voronoi diagrams³ (Fig. 1). It is important to note that all the processing and detection steps were fully automatized. The only significant intervention of the grader was the placement of the square, which determines the measurement area. Because of the resolution limits of the camera (250 line pairs per millimetre), it was not possible to differentiate cones inside a circle of 1° of radius where cells are too tightly packed,³¹ with a risk of underestimating the cone density in the very centre of the fovea. (Fig. 1) For this reason, the area of analysis chosen in this study corresponded to a $90\text{-}\mu\text{m}$ square ($0.3^\circ \times 0.3^\circ$), placed 1.5° nasally from the fovea by the grader, on the horizontal axis

Figure 1. Preprocessed and postprocessed adaptive optics (AO) images. (a) Preprocessed AO image of a right eye centred on 0° ($4^\circ \times 4^\circ$). Cones in the very centre appear blurred because of resolution limitation of the AO camera. Analysis provided by AOdetect 0.1 software: (b) color map representing spacing between cones; (c) cone density map; (d) Voronoi diagram representing the distribution of neighbouring cones. Color scales are presented at the bottom.



crossing the fovea. The square was manually moved along the horizontal axis following a 10-μm step until reaching the highest density detected along this axis (Fig. 2).

In order to adjust the scale of the retinal images, axial length was obtained using the IOL Master (Carl Zeiss Meditec, Dublin, CA, USA).

Study design

All eyes studied were right eyes. Sessions were conducted in the same low-lighting conditions, using the same retinal camera.

Intrasession repeatability was measured by comparing 10 consecutive images acquired by the same operator from three different subjects. Cone counts were performed by the same grader, using AOdetect v0.1.

Intersession reproducibility was assessed by comparing the images obtained from three subjects, on five consecutive days, by the same operator and the same grader.

Interoperator reproducibility was measured by imaging 10 subjects by two operators in a blinded manner, in the same conditions (same device, same examination time, same lighting).

Intergrader reproducibility was assessed by comparing the results of cone counts obtained from 60 different images measured by two masked graders.

Statistical analysis

The averaged cone densities, spacings and P6, the standard deviations and the confidence intervals (CI) were calculated for each part of the study. Descriptive statistics and the Wilcoxon matched-pairs signed-ranks test were used for statistical comparisons between groups, with the two-tail *P* value ≤ 0.05 considered significant.

The degree of agreement between the two operators and between the two readers was assessed using the Bland-Altman method.³²⁻³⁴ The standard deviation of repeated measurements enables to

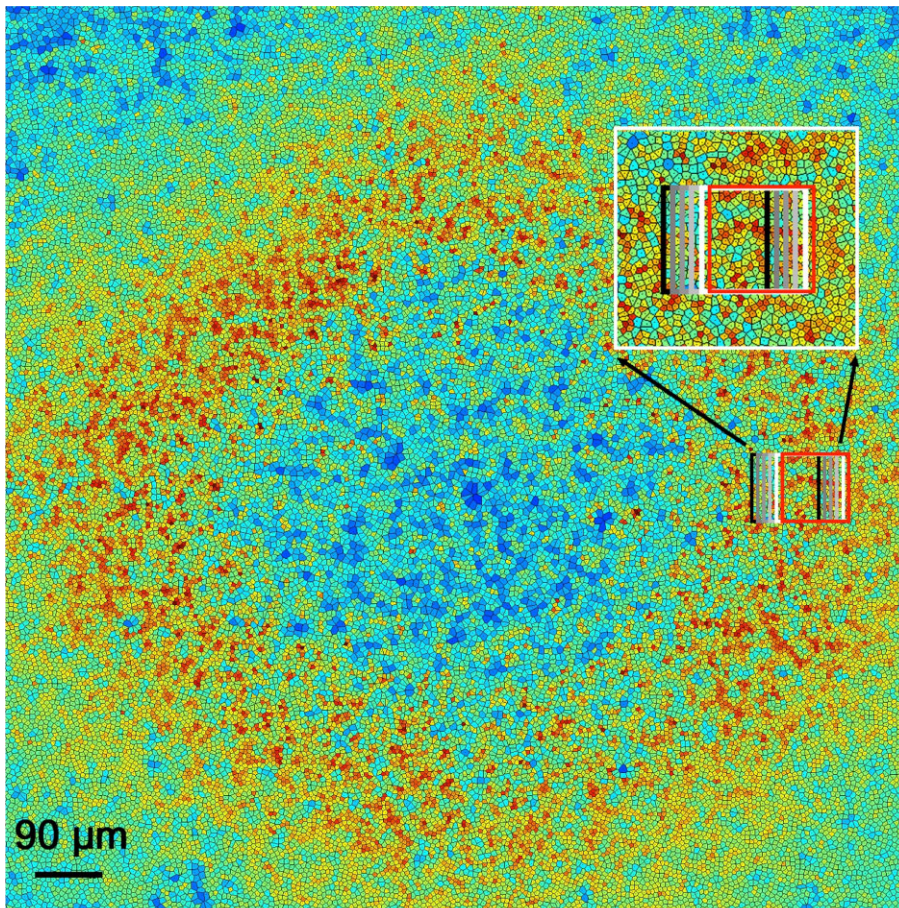
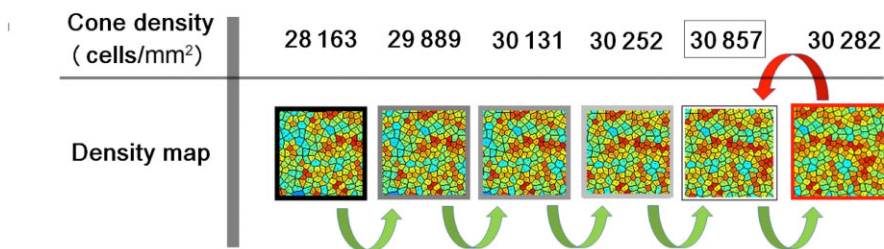


Figure 2. Illustration of the cone-counting method on the nasal area along a horizontal line passing through the foveola (right eye). (a) Cone density map obtained by AOdetect software. A $0.3^\circ \times 0.3^\circ$ ($90 \mu\text{m} \times 90 \mu\text{m}$) square is moved manually along the horizontal line starting at the center with a step of $10 \mu\text{m}$ until reaching the highest cone density detected. When the cone density starts to decrease (red square), the square is moved backward to the previous area. The corresponding density, spacing and percentage of cells with six neighbours are then reported. (b) Image cone labelling process in the $0.3^\circ \times 0.3^\circ$ square, with the automated algorithm provided by AOdetect 0.1 software. Red crosses represent cones identified by the algorithm.



measure the size of the measurement error. The common standard deviation of repeated measurements is known as the within-subject standard deviation, S_w , as described by Bland and Altman in 1996.³² To estimate S_w , the variances (the squares of the standard deviations) are averaged. The difference between a subject's measurement and the true value would be expected to be less than $1.96 S_w$, for 95% of observations. Repeatability is another way to present measurement error. It is defined as $2.77 S_w$. The difference between two measurements for the same subject is expected to be less than $2.77 S_w$, for 95% of pairs of observations.³²⁻³⁴ The 95% CI for repeatability is $1.96 S_w / \sqrt{(2n(m-1))}$ where n is the number of subjects and m is the number of observations for each subject.

For test-retest analysis, coefficients of variation, correlation coefficients (CCs) and intraclass CCs were

calculated. Coefficients of variation are a measure of dispersion of a distribution, ratio of the standard deviation to the mean. CCs describe the correlation between two variables, but they may be difficult to interpret because this correlation depends on the variability between subjects. So intraclass CCs were also reported. Intraclass CCs estimate the average correlation between all possible pairs of observation.³⁴

Statistics were calculated using the commercially available software program GraphPad InStat (GraphPad InStat, Inc., San Diego, CA, USA). Linear regression graphs were obtained using Graph Prism 5 (GraphPad InStat, Inc.).

RESULTS

The characteristics of the 10 volunteers studied are reported in Table 1.

Intra- and intersession studies

Intrasession and intersession test results are summarized in Tables 2 and 3.

Intrasession repeatability was good for the overall parameters studied. Cone spacing appeared to be the

most reproducible parameter. There was a decreasing trend in cone detection over the duration of the session. However, it did not reach a level of statistical significance (data not shown). Intersession reproducibility was also good for cone density and cone spacing measurements and to a lesser degree for P6.

Table 1. Characteristics of the studied volunteers

Demographic characteristics	
Age (years) Mean (95%CI) SD	30.80 (25.99,35.61) 6.73
Spherical equivalent (diopters) Mean (95%CI) SD	-1.05 (-2.62,0.52) 0.69
Sex ratio	1

CI, confidence interval; SD, standard deviation.

Interoperator study

The results of the interoperator study are summarized in Table 4. Interoperator agreement was consistent for cone density and cone spacing, but not for P6. The Bland–Altman analysis showed a mean difference among operators of 772.4 cells/mm² (Fig. 3), 0.086 μ m for spacing and 0.34% for P6.

Table 2. Intrasession repeatability

Subjects	Density			Spacing			P6		
	Mean cells/mm ² (95%CI) (Range)	SD	COV %	Mean μ m (95%CI) (Range)	SD	COV %	Mean % (95%CI) (Range)	SD	COV %
Subject 1	23 914 (22 839, 24 989) (21 174 to 26 016)	1503	6.29	7.19 (7.04, 7.34) (6.90 to 7.56)	0.20	2.92	39.38 (37.42, 41.34) (34.40 to 43.90)	2.73	6.94
Subject 2	29 058 (27 846, 30 270) (24 432 to 30 644)	1695	5.83	6.49 (6.31, 6.66) (6.27 to 7.13)	0.24	3.71	46.31 (42.98, 49.64) (39.10 to 56.8)	4.65	10.05
Subject 3	23 962 (23 045, 24 879) (22 716 to 26 350)	1282	5.35	7.16 (7.04, 7.28) (6.89 to 7.36)	0.16	2.37	42.81 (40.39, 45.23) (37.80 to 49.10)	3.38	7.90
Overall patients	25 644 (24 580, 26 709) (21 174 to 30 644)	2851	5.82	6.95 (6.81, 7.10) (6.27 to 7.56)	0.39	3	42.83 (41.13, 44.54) (34.40 to 56.80)	4.57	8.30

CI, confidence interval; COV, coefficient of variation; P6, percentage of cells with six neighbours; SD, standard deviation.

Table 3. Intersession reproducibility

Subjects	Density			Spacing			P6		
	Mean cells/mm ² (95%CI) (Range)	SD	COV %	Mean μ m (95%CI) (Range)	SD	COV %	Mean % (95%CI) (Range)	SD	COV %
Subject 1	22 807 (20 270, 25 344) (20 659 to 25 378)	2043	8.96	7.37 (6.99, 7.75) (7.02 to 7.78)	0.30	4.12	40.44 (37.10, 43.78) (37.20 to 44.40)	2.69	6.66
Subject 2	28 690 (27 860, 30 060) (27 398 to 29 443)	910	3.17	6.58 (6.44, 6.71) (6.47 to 6.71)	0.11	1.66	43.92 (38.79, 49.05) (39.80 to 50.20)	4.13	9.40
Subject 3	24 204 (22 767, 25 640) (22 572 to 25 839)	1157	4.78	7.12 (6.85–7.40) (6.86 to 7.46)	0.22	3.09	40.68 (38.74, 42.62) (39.00 to 42.90)	1.56	3.85
Overall Patients	25 233 (23 613, 26 854) (20 659 to 29 443)	2925	5.63	7.02 (6.80, 7.25) (6.47 to 7.78)	0.40	2.96	41.68 (39.90, 43.46) (37.20 to 50.20)	3.22	6.64

CI, confidence interval; COV, coefficient of variation; P6, percentage of cells with six neighbours; SD, standard deviation.

Table 4. Results of the interoperator study

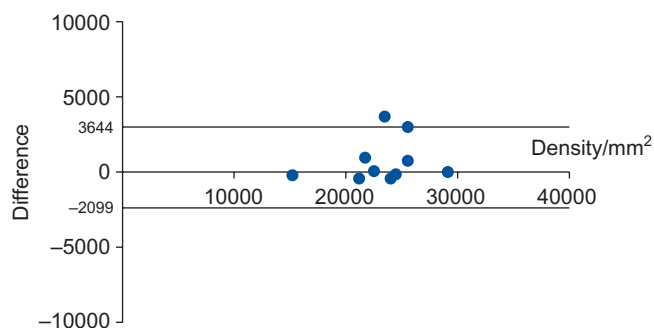
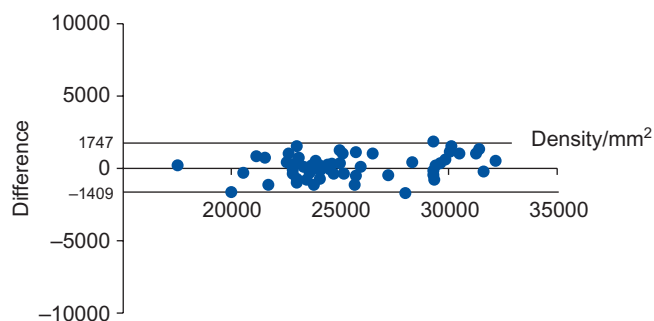
Correlation coefficients	Density	Spacing	P6
Intraclass CC % (95%CI)	0.96 (0.83, 0.99)	0.96 (0.85, 0.99)	0.20 (-2.19, 0.80)
Correlation coefficient %	0.81	0.94	0.12

CC, correlation coefficient; CI, confidence interval; P6, percentage of cells with six neighbours.

Table 5. Results of the intergrader study

Correlation coefficients	Density	Spacing	P6
Intraclass CC % (95%CI)	0.98 (0.976, 0.0.991)	0.96 (0.943, 0.980)	0.78 (0.634, 0.869)
Correlation coefficient %	0.97	0.95	0.61

CC, correlation coefficient; CI, confidence interval; P6, percentage of cells with six neighbours.

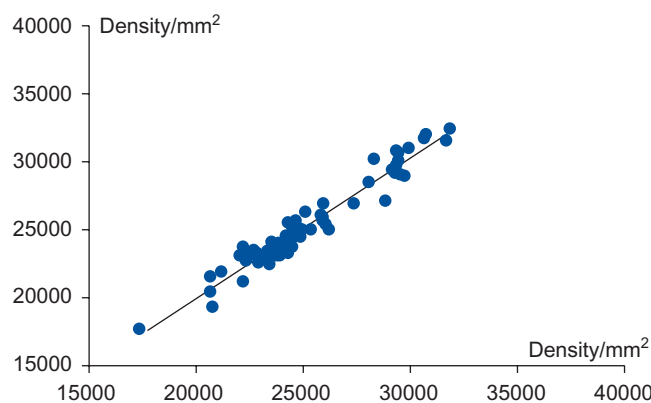
**Figure 3.** Bland–Altman graph representing interoperator reproducibility of cone density. Gray lines correspond to the 95% confident interval of the difference between the two operators.**Figure 4.** Bland–Altman graph representing the intergrader agreement in cone counts. Gray lines correspond to the 95% confident interval of the difference between the two readers.

Intergrader agreement

Intergrader reproducibility was high for cone density and cone spacing but was again limited for P6 (Table 5). The Bland–Altman analysis for intergrader agreement showed a mean difference among graders of 169.4 cells/mm² (Fig. 4), 0.003 μ m for spacing and 0.24% for P6. As for the linear regression between the cone density measured by the two blinded graders, R^2 was 0.95 (Fig. 5).

DISCUSSION

This study provides an estimate of the reproducibility of RTX-1-derived cone counts in the ideal setting for imaging cones. Overall, there was a good repro-

**Figure 5.** Relation between the cone density measured in 60 images by two blinded graders (linear regression, $R^2 = 0.95$).

ducibility across results for parafoveal cone density and for the inter-cone spacing measurements, and to a lesser degree for the percentage of cones with six neighbours. Garrioch *et al.* reported in 2012, results of cone counts with their self-built AO device, coupled with a SLO.²⁵ They found a high variability in cone counts with automated estimates with a coefficient of repeatability of 17.1%. However, optimization of the identification software combined with complementary manual identification of cones missed by the automated algorithm improved the results considerably, to up to 2.7%. The current study, which focused on the first commercially available device, differs in several points from the latter: the wavelength of the super-luminescent diode used for retinal imaging was 850 nm for the RTX-1 versus 775 nm for the AOSLO device. The subtending field of view of the RTX-1 was four times wider. The software provided by the manufacturer was based on specific algorithms designed to detect cones and protected by several patents. In consequence, it was not possible to modify the automatic count by adding or subtracting elements involved in the cell count. In addition, the cone-counting protocol implemented in the current study was original. While the Wisconsin team imaged the cones at 0.65° from the centre of fixation, we studied the area located at 1.5° for the technical reason indicated earlier. Despite a different approach, we found good repeatability and reproducibility of both the optical system and its software

with test–retest coefficients of variation under 7%. The variability observed between the measurements may have several origins. The capacity of the subject to stay focused on the fixation target was important because each acquisition lasted 4 s. Interestingly, during the intrasession study, there was a downward trend in cone density values as the session progressed, although the difference did not reach statistical significance. Most likely, the decrease in image resolution, which was responsible for a loss of cell detection, was caused by progressive impairment of the tear film resulting in increased optical aberrations. Another factor of variation was the nature of the cone-counting procedure. The process was not fully automated because the area of analysis for cone count was selected manually, which contributed greatly to the overall amount of variation, as demonstrated in the intergrader study. A software upgrade to automatically detect the parafoveal cone peak in a preselected area would certainly improve the accuracy of the cone counts. Interoperator agreement was also good because both operators were well trained and followed the same acquisition protocol. However, results with less experienced operators may display a higher variability.

This study has limitations. The major one is that it was voluntarily conducted on normal eyes selected to minimize potential optical defects that could influence AO image quality. In a normal clinical setting, impaired tear film, cataract and fixation difficulties, among other factors, may accentuate the differences observed between measurements in normal eyes. However, their impact on the measurements is difficult to quantify precisely and it would have been very difficult to distinguish between what is due to the imaging system and what is related to the disease by itself. Another point is that the cone count is entirely based on the identification of cones by the algorithm of the software. The recognition elements included shape, size and reflectivity. In absence of comparison with the gold standard, which would have been histological sampling, it is not possible to confirm the accuracy of the results obtained by the software. Nevertheless, the cone-count protocol we implemented focused on a small nasal area where cones make up, by far, the majority of cells³¹ minimizing the risk of confusion between different cell types. The RTX-1 provides images with a lateral resolution of approximately 3 μm and accurately measures macular cone density and mosaic in the eight central degrees but not in the very centre of the fovea (< 1 central degree) where the cones cannot be discriminated due to their small size and their high density in this area (up to 200 000 cells/ mm^2).³¹ In our opinion, detecting the parafoveal cone peak instead of counting cones at a fixed distance from the fovea is more relevant for clinical applications, in

order to draw comparison between patients because the spatial distribution of macular cones can differ between individuals. In fact, Curcio *et al.*^{31,35} described several patterns of cone distribution in histological observations, from circular to oval shapes that makes it more difficult to compare individuals at a fixed distance from the fovea.

Another notable difference between AO studies resides in the sampling window size. With AOSLO, a decrease in the repeatability and an increase in the measurement error of cone density were observed as the square size decreased.²⁵ The same effect was reported in the Lombardo *et al.* study, which assessed the agreement between sampling windows of different sizes (320 \times 160 μm , 160 \times 80 μm and 80 \times 40 μm) acquired in 10 subjects, at 1.20° nasally and 1.70° temporally from the centre of fixation, using a RTX-1 device.³⁶ Besides, the closer to the fovea the area of measurement is, the higher the intersubject variability is.^{3,24,31} The results of the current study are comparable with those already reported in the literature, with an average coefficient of repeatability of the same order of magnitude as the one reported by Lombardo *et al.*, which was close to 10%.³⁶

Finally, it appears that, at the current stage, RTX-1 does not detect a narrow difference in cone counts (<10%) with a sufficient degree of confidence. These results underline the need for exercising caution when interpreting the results of future studies concluding on very slight differences in cone density, especially when the lower limit of cone counts possibly expressing a clinical symptom remains unknown to date. We are currently assessing the device reliability in specific group of patients in order to contribute to define the best clinical application of this promising imaging modality.

In conclusion, cone counts using RTX-1 appeared reliable over time, in healthy volunteers, to a certain limit. Further studies in various retinal conditions are mandatory in order to implement their use in routine ophthalmology.

REFERENCES

1. Liang J, Williams DR, Miller DT. Supernormal vision and high-resolution retinal imaging through adaptive optics. *J Opt Soc Am A Opt Image Sci Vis* 1997; **14**: 2884–92.
2. Chui TYP, Song H, Burns SA. Adaptive-optics imaging of human cone photoreceptor distribution. *J Opt Soc Am A Opt Image Sci Vis* 2008; **25**: 3021–9.
3. Li KY, Tiruveedhula P, Roorda A. Intersubject variability of foveal cone photoreceptor density in relation to eye length. *Invest Ophthalmol Vis Sci* 2010; **51**: 6858–67.
4. Lombardo M, Serrao S, Ducoli P, Lombardo G. Variations in image optical quality of the eye and the sampling limit of resolution of the cone mosaic with axial length in young adults. *J Cataract Refract Surg* 2012; **38**: 1147–55.

5. Lombardo M, Lombardo G, Schiano LD, Ducoli P, Stirpe M, Serrao S. Interocular symmetry of parafoveal photoreceptor cone density distribution. *Retina* 2013; **33**: 1640–9.
6. Lombardo M, Serrao S, Ducoli P, Lombardo G. Eccentricity dependent changes of density, spacing and packing arrangement of parafoveal cones. *Ophthalmic Physiol Opt* 2013; **33**: 516–26.
7. Park SP, Chung JK, Greenstein V, Tsang SH, Chang S. A study of factors affecting the human cone photoreceptor density measured by adaptive optics scanning laser ophthalmoscope. *Exp Eye Res* 2012; **108**: 1–9.
8. Lombardo M, Scarinci F, Ripandelli G *et al.* Adaptive optics imaging of idiopathic epiretinal membranes. *Ophthalmology* 2013; **120**: 1508–9.
9. Ooto S, Hangai M, Takayama K *et al.* High-resolution imaging of the photoreceptor layer in epiretinal membrane using adaptive optics scanning laser ophthalmoscopy. *Ophthalmology* 2011; **118**: 873–81.
10. Ooto S, Hangai M, Takayama K, Ueda-Arakawa N, Hanebuchi M, Yoshimura N. Photoreceptor damage and foveal sensitivity in surgically closed macular holes: an adaptive optics scanning laser ophthalmoscopy study. *Am J Ophthalmol* 2012; **154**: 174–86.
11. Yokota S, Ooto S, Hangai M *et al.* Objective assessment of foveal cone loss ratio in surgically closed macular holes using adaptive optics scanning laser ophthalmoscopy. *PLoS ONE* 2013; **8**: e63786.
12. Gocho-Nakashima K, Benchaboune M, Ullern M *et al.* Adaptive optics imaging in age-related macular degeneration. *Acta Ophthalmol (Copenh)* 2011; **89**: 0. doi: 10.1111/j.1755-3768.2011.4111.x
13. Gocho K, Sarda V, Falah S *et al.* Adaptive optics imaging of geographic atrophy. *Invest Ophthalmol Vis Sci* 2013; **54**: 3673–80.
14. Zayit-Soudry S, Duncan JL, Syed R, Menghini M, Roorda AJ. Cone structure imaged with adaptive optics scanning laser ophthalmoscopy in eyes with nonneovascular age-related macular degeneration. *Invest Ophthalmol Vis Sci* 2013; **54**: 7498–509.
15. Koozekanani D, Roberts C, Katz SE, Herderick EE. Intersession repeatability of macular thickness measurements with the Humphrey 2000 OCT. *Invest Ophthalmol Vis Sci* 2000; **41**: 1486–91.
16. Muscat S, McKay N, Parks S, Kemp E, Keating D. Repeatability and reproducibility of corneal thickness measurements by optical coherence tomography. *Invest Ophthalmol Vis Sci* 2002; **43**: 1791–5.
17. Muscat S, Parks S, Kemp E, Keating D. Repeatability and reproducibility of macular thickness measurements with the Humphrey OCT system. *Invest Ophthalmol Vis Sci* 2002; **43**: 490–5.
18. Polito A, Del Borrello M, Isola M, Zemella N, Bandello F. Repeatability and reproducibility of fast macular thickness mapping with stratus optical coherence tomography. *Arch Ophthalmol* 2005; **123**: 1330–7.
19. Garcia-Martin E, Pinilla I, Idoipe M, Fuertes I, Pueyo V. Intra and interoperator reproducibility of retinal nerve fibre and macular thickness measurements using Cirrus Fourier-domain OCT. *Acta Ophthalmol (Copenh)* 2011; **89**: e23–9.
20. Rahman W, Chen FK, Yeoh J, Patel P, Tufail A, Da Cruz L. Repeatability of manual subfoveal choroidal thickness measurements in healthy subjects using the technique of enhanced depth imaging optical coherence tomography. *Invest Ophthalmol Vis Sci* 2011; **52**: 2267–71.
21. Savini G, Carbonelli M, Parisi V, Barboni P. Repeatability of optic nerve head parameters measured by spectral-domain OCT in healthy eyes. *Ophthalmic Surg Lasers Imaging* 2011; **42**: 209–15.
22. Yamashita T, Yamashita T, Shirasawa M, Arimura N, Terasaki H, Sakamoto T. Repeatability and reproducibility of subfoveal choroidal thickness in normal eyes of Japanese using different SD-OCT devices. *Invest Ophthalmol Vis Sci* 2012; **53**: 1102–7.
23. Talcott KE, Ratnam K, Sundquist SM *et al.* Longitudinal study of cone photoreceptors during retinal degeneration and in response to ciliary neurotrophic factor treatment. *Invest Ophthalmol Vis Sci* 2011; **52**: 2219–26.
24. Song H, Chui TYP, Zhong Z, Elsner AE, Burns SA. Variation of cone photoreceptor packing density with retinal eccentricity and age. *Invest Ophthalmol Vis Sci* 2011; **52**: 7376–84.
25. Garrioch R, Langlo C, Dubis AM, Cooper RF, Dubra A, Carroll J. Repeatability of in vivo parafoveal cone density and spacing measurements. *Optom Vis Sci* 2012; **89**: 632–43.
26. Zitova B, Flusser J. Image registration methods: a survey. *Image Vis Comput* 2003; **21**: 977–1000.
27. Kulcsar C, Le Besnerais G, Ödlund E, Levecq X. *Robust Processing of Image Sequences Produced by an Adaptive Optics Retinal Camera*. Arlington, TX: OSA, 2013.
28. Kuan DT, Sawchuk AA, Strand TC, Chavel P. Adaptive noise smoothing filter for images with signal-dependent noise. *IEEE Trans Pattern Anal Mach Intell* 1985; **7**: 165–77.
29. Lindeberg T. *Scale-Space Theory in Computer Vision*. Boston/London/Dordrecht: Kluwer Academic Publishers, 1993.
30. De Berg M, Van Kreveld M, Overmars M, Schwarzkopf OC. *Computational Geometry: Algorithms and Applications*, 2nd revised edn. Berlin, Heidelberg and New York: Springer, 2000.
31. Curcio CA, Sloan KR, Kalina RE, Hendrickson AE. Human photoreceptor topography. *J Comp Neurol* 1990; **292**: 497–523.
32. Bland JM, Altman DG. Statistics notes: measurement error. *BMJ* 1996; **312**: 1654.
33. Bland JM, Altman DG. Measurement error proportional to the mean. *BMJ* 1996; **313**: 106.
34. Bland JM, Altman DG. Measurement error and correlation coefficients. *BMJ* 1996; **313**: 41–2.
35. Curcio CA, Sloan KR. Packing geometry of human cone photoreceptors: variation with eccentricity and evidence for local anisotropy. *Vis Neurosci* 1992; **9**: 169–80.
36. Lombardo M, Serrao S, Ducoli P, Lombardo G. Influence of sampling window size and orientation on parafoveal cone packing density. *Biomed Opt Express* 2013; **4**: 1318–31.